

## Fermi-hypernetted-chain scheme for Gutzwiller correlated wave functions

X. Q. G. Wang

*International School for Advanced Studies, 34014 Trieste, Italy*

S. Fantoni

*International School for Advanced Studies and Istituto Nazionale de Fisica Nucleare, Sezione di Trieste, 34014 Trieste, Italy*

E. Tosatti

*International School for Advanced Studies, 34014 Trieste, Italy  
and International Centre for Theoretical Physics, 34100 Trieste, Italy*

L. Yu

*International Centre for Theoretical Physics, 34100 Trieste, Italy  
and Institute of Theoretical Physics, Academia Sinica, 100080 Beijing, China*

(Received 18 January 1994)

A set of integral equations in the Fermi-hypernetted-chain scheme is formulated for Gutzwiller correlated wave functions. The well-known exact analytical results of Vollhardt, Metzner, and Gebhard for the one- and infinite-dimensional Gutzwiller paramagnetic wave functions are recovered as a byproduct of the theory. In approximate form, the theory is applicable to arbitrary Gutzwiller correlated wave functions, irrespective of the space dimensionality of the model.

Recently, the conventional Fermi-hypernetted-chain (FHNC) theory has been generalized to treat lattice models, and used to perform variational calculations for the one-dimensional (1D) and 2D Hubbard model at  $T = 0$ , with various types of trial wave functions possessing either paramagnetic (PM), spin-density-wave (SDW), or BCS symmetry properties.<sup>1,2</sup> It has been found that the FHNC provides reliable estimates of the pair-correlation function and the momentum distribution only for weak and intermediate values of the coupling constant  $U/t \leq 6$ .<sup>2</sup> No direct connections were found between the FHNC approximations and the exact solutions for one and infinite dimensions found by Vollhardt and co-workers.<sup>3,4</sup>

The FHNC theory provides the technological background necessary to perform correlated-basis-function (CBF) perturbative calculations, extensively applied in the studies of strongly interacting continuous systems, such as liquid helium and nuclear matter.<sup>5,6</sup> CBF calculations constitute an interesting alternative to stochastic calculations, such as quantum Monte Carlo<sup>7</sup> or green-function Monte Carlo,<sup>8</sup> which still suffer from the *fermion-sign problem*, and exact diagonalization,<sup>9</sup> limited to small systems.

The CBF theory requires evaluating nondiagonal matrix elements of the Hamiltonian and the unity operators on CBF states  $|\Psi_n\rangle = \hat{F}|\Phi_n\rangle$ , where  $|\Phi_n\rangle$  are mean-field states and  $\hat{F}$  a correlation operator. Such calculations, at present, cannot be carried out by Monte Carlo sampling, which is instead successfully applied to compute expectation values on  $|\Psi_0\rangle$ .<sup>10</sup> Therefore, the FHNC technologies need to be further developed for lattice systems in order to be applicable for a wide range of the Hubbard coupling constant.

In this paper, we show that for the particular class of

Gutzwiller correlated wave functions the FHNC theory can be recast in a form which, on the one hand, allows one to easily recover the well-known exact solutions for one and infinite dimensions<sup>3,4</sup> and, on the other hand, suggests suitable *scaling* approximations providing very good results as tested in 1D and 2D for a wide range of the coupling constant  $U/t$ .

The on-site character of the Gutzwiller correlation operator

$$\hat{F}_G = \prod_i [1 - (1-g)\hat{n}_{i\uparrow}\hat{n}_{i\downarrow}] = \prod_{i<j} [1 - (1-g)\delta_{\mathbf{r}_i\uparrow\mathbf{r}_j\downarrow}], \quad (1)$$

implies that the FHNC diagrammatic structures displayed in Fig. 1 correspond to configurations which are Pauli violating: (i) the *star structure* of diagram

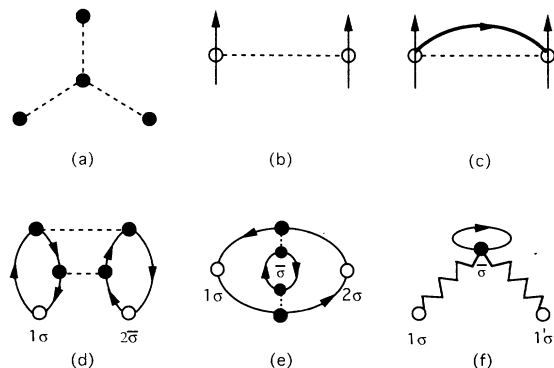


FIG. 1. Diagrammatic structures in GHNC theory: (a-c) are forbidden structures; (d,e) are GHNC diagrams contributing to the pair function and (f) to the density matrix.

(a), where two or more dynamical correlators  $\hat{h}(i, j) = (g^2 - 1)\delta_{\mathbf{r}_i, \mathbf{r}_j}$  (represented by a dashed line joining the points  $i$  and  $j$ ) have a single common particle label, and therefore imply three or more particles on the same site; (ii) the *correlated parallel spin structure* of diagrams (b) and (c), where the correlator  $\hat{h}(i, j)$  implies that the two particles with the same spin assignment occupy the same site.

All diagrams containing the above structures are bound to give spurious contributions. They cancel each other only after an exact FHNC summation. This implies that the various FHNC approximations, like, e.g., FHNC/n or FHNC-n,<sup>2</sup> corresponding to different ways of truncating the FHNC cluster series, suffer from this problem which becomes more and more severe for increasing coupling constant in the Hubbard Hamiltonian. Therefore a better chain summation method should sum up only the *nonspurious* diagrams, hereafter referred to as GHNC (Gutzwiller-hypernetted-chain) diagrams.

The GHNC diagrams, contributing to the pair-correlation function  $\tilde{g}(\mathbf{r}_{12})$ , are characterized by the property that each point is reached by one and only one correlation line, except for the two external points 1 and 2, which do not need to be reached by a correlation line. As a general property,<sup>5</sup> each point has also to be reached by one incoming and one outgoing oriented solid line representing the *exchange correlation operator*  $\hat{\rho}_\sigma(i, j) = \sum_{\mathbf{k} \in \text{Fermi sea}} \varphi_{\mathbf{k}\sigma}^\dagger(i) \varphi_{\mathbf{k}\sigma}(j)$ , where  $\varphi_{\mathbf{k}\sigma}(i)$  are the single-particle states entering  $|\Phi_0\rangle$ . The exchange lines form closed loops (one-point loops are often omitted in FHNC diagrams in the case of spin-independent correlations). Since all particles belonging to the same exchange loop must have the same spin assignment, it follows that any two points cannot be joined by both dynamical and exchange correlations [see diagram (c) of Fig. 1].

The removal of the Pauli violating diagrams implies that the reducibility theorem of FHNC theory<sup>5,6</sup> does not apply anymore and therefore *the GHNC reducible diagrams do not cancel each other*.

In the case of the one-body density matrix  $\hat{n}(\mathbf{r}_1, \mathbf{r}_{1'})$ , since  $\mathbf{r}_1$  and  $\mathbf{r}_{1'}$  both correspond to the same particle 1, one finds that (i) there is one open exchange pattern going from 1 to 1'; (ii) the correlation reaching either 1 or 1' are given by  $\hat{\xi}(i, j) = (g - 1)\delta_{\mathbf{r}_i, \mathbf{r}_j}$  instead of  $\hat{h}(i, j)$ ; (iii) the *star structure*  $\hat{\xi}(1, i)\hat{\xi}(i, 1')$  is allowed.

The structure of the GHNC diagrams is independent of the particular reference state  $|\Phi_0\rangle$  considered (like PM, SDW, etc.) and of the dimensionality. A few examples of GHNC diagrams for the pair distribution function and

the one-body density matrix are displayed in Fig. 1 [diagrams (d)–(f)].

Let us now discuss the properties of the GHNC diagrams in the case of the 1D model with a Gutzwiller correlated PM reference state.

The on-site character of  $\hat{h}(i, j)$  implies that, after the  $r$ -space integration, all dashed lines shrink to points, each carrying a factor  $(g^2 - 1)$ . It follows that the double occupancy  $d = \langle \hat{n}_{i\uparrow} \hat{n}_{i\downarrow} \rangle$  is given by<sup>11</sup>

$$d \equiv \tilde{g}(\mathbf{r}_{ij} = 0) = g^2 \sum_{m=0}^{\infty} C_m [(g^2 - 1)]^m, \quad (2)$$

where  $C_m$  sums up contributions from all GHNC diagrams having  $2m$  internal points. In the 1D-PM case, the exchange correlation operator has a simple structure<sup>2</sup>  $\hat{\rho}_\sigma(i, j) = \eta^\dagger(\sigma_i)\eta(\sigma_j)\rho_\sigma l(k_F^\sigma x_{ij})$ , where  $\eta(\sigma)$  is the spin state and  $l(k_F^\sigma x_{ij}) = \sin k_F^\sigma x_{ij} / (k_F^\sigma x_{ij})$ ,  $k_F^\sigma = \pi\rho_\sigma$  being the Fermi momentum for spin- $\sigma$  component. As a consequence, the structure of a generic term, in the case of  $\rho_\sigma = \rho_{\bar{\sigma}} = \rho/2$ , contributing to  $C_m$  is given by  $\rho_\sigma^{2m+2} \int \prod_{i=3}^{m+2} dx_i \{\text{products of } l(k_F^\sigma x_{ij})\}$ , which is just proportional to  $\rho^{m+2}$ , as one can see by changing variables  $x_i$  into  $k_F^\sigma x_i$  in the integral. Using this property and the particle-hole ( $p$ - $h$ ) symmetry one recovers the exact solution originally found by Metzner and Vollhardt,<sup>3</sup>

$$C_m = (-1)^{m+2} \frac{\rho^{m+2}}{2(m+2)}, \quad m \geq 0. \quad (3)$$

Similar arguments can be used to get the exact expression of the momentum distribution, and other correlation functions.<sup>12</sup> The crucial ingredient of this 1D exact summation is the  $p$ - $h$  symmetry.

In a more general case,  $p$ - $h$  symmetry cannot be used to get an exact analytical result, and the GHNC diagrams need to be summed up explicitly.

A structural analysis of the GHNC diagrams shows<sup>2</sup> that they can be summed by integral equations using a two-body *propagator*  $\hat{G}_{cc\sigma}(i, j)$  and a four-body kernel  $\hat{\Gamma}_{\sigma\sigma'}(i, j; i', j')$  as functional variables.  $\hat{G}_{cc\sigma}(i, j)$  behaves like a dressed exchange operator and obeys the chain-type equation

$$\hat{G}_{cc\sigma}(i, j) = -\hat{\rho}_\sigma(i, j) - \sum_{i,l} \hat{\rho}_\sigma(i, k) \hat{\Sigma}_\sigma^*(k, l) \hat{G}_{cc\sigma}(l, j), \quad (4)$$

where the quantity  $\hat{\Sigma}_\sigma^*(k, j)$  corresponds to the sum of *proper self-energy* GHNC diagrams, calculated from

$$\hat{\Sigma}_\sigma^*(i, j) = (1 - g^2) \left[ \delta(\mathbf{r}_{ij}) \hat{G}_{cc\bar{\sigma}}(i, j) + \sum_{i', k, k'} \hat{\Gamma}_{\sigma\bar{\sigma}}(i, k; i', k') \hat{G}_{cc\bar{\sigma}}(i', j) \hat{G}_{cc\bar{\sigma}}(j, k) \hat{G}_{cc\sigma}(k', j) \right], \quad (5)$$

where the first term in the square bracket is related to vertex corrections, while the second term is due to other than chain GHNC diagrams. With  $\hat{\Gamma}_{\sigma\sigma'}^{(ir)}$  as its irreducible part,  $\hat{\Gamma}_{\sigma\bar{\sigma}}$  satisfies a Bethe-Salpeter equation:

$$\hat{\Gamma}_{\sigma\sigma'}(i, j; i', j') = \hat{\Gamma}_{\sigma\sigma'}^{(ir)}(i, j; i', j') - \sum_{i'', j''; i''', j'''; \sigma''} \hat{\Gamma}_{\sigma\sigma''}^{(ir)}(i, j; i'', j'') \hat{G}_{cc\sigma''}(i'', i''') \hat{G}_{cc\sigma''}(j'', j''') \hat{\Gamma}_{\sigma''\sigma'}(i''', j'''; i', j'). \quad (6)$$

Alternatively, one can write a set of three integral equations involving two-body quantities only, hereafter referred to as GHNC equations, which closely resemble the FHNC equations and whose derivation is a straightforward application of the FHNC theory to the GHNC diagrams. The full expressions of the GHNC equations, as well as of quantities related to  $\hat{\Sigma}_\sigma^*$  and  $\hat{\Gamma}_{\sigma\sigma'}^{(ir)}$  appearing in Eqs. (4,6) are cumbersome, and will be given in detail elsewhere.<sup>12</sup> Obviously, the elementary diagrams in GHNC equations, as well as those occurring in  $\hat{\Gamma}_{\sigma\sigma'}^{(ir)}$  cannot in general be calculated in a closed form, except by using some global property, e.g., the  $p$ - $h$  symmetry in the 1D PM case. Hence the two schemes expressed either by Eqs. (4,6) or by the GHNC equations are intrinsically approximate and differ by the way the elementary diagrams are included in the iterative procedure. For instance, the simplest structure of  $\hat{\Gamma}_{\sigma\sigma'}^{(ir)}$ , e.g.,  $\delta_{i,i'}\delta_{j,j'}\hat{h}(i,j)$ , already implies the inclusion of a large class of elementary diagrams in the GHNC equations.

A remarkable property following from the structure of the GHNC diagrams is that both the double occupancy  $d$  and the momentum distribution  $n_\sigma(\mathbf{k}) = \langle \hat{c}_{\mathbf{k}\sigma}^\dagger \hat{c}_{\mathbf{k}\sigma} \rangle$  can be expressed in terms of  $\hat{\Sigma}_\sigma^*(\mathbf{k})$  only. For the PM wave function one has<sup>12</sup>

$$d = \frac{g^2}{g^2 - 1} \sum_{\mathbf{k}} \frac{\hat{\Sigma}_\sigma^*(\mathbf{k})}{1 + \hat{\Sigma}_\sigma^*(\mathbf{k})} \theta(|\mathbf{k}_F^\sigma - \mathbf{k}|), \quad (7)$$

and

$$n_\sigma(\mathbf{k}) = \frac{1}{1 + \hat{\Sigma}_\sigma^*(\mathbf{k})} \left[ \frac{1 + g + \hat{\Sigma}_\sigma^*(\mathbf{k})}{1 + g} \right]^2 \theta(|\mathbf{k}_F^\sigma - \mathbf{k}|) + \frac{1}{(g+1)^2} [\rho_\sigma(g^2 - 1) - \hat{\Sigma}_\sigma^*(\mathbf{k})]. \quad (8)$$

It is well known that the two-body elementary diagrams are short-range functions.<sup>6</sup> Assuming their main contribution to be on site, we propose the following approximation for the elementary diagrams contributing to  $\hat{\Sigma}_\sigma^*(\mathbf{k})$ :

$$\hat{\Sigma}_\sigma^*(\mathbf{k}) = \hat{\Sigma}_\sigma^{\text{GHNC}}(\mathbf{k}) + \hat{\mu}_\sigma \quad (9)$$

where  $\hat{\Sigma}_\sigma^{\text{GHNC}}$  is calculated by solving the GHNC equations at a given level of approximation for the elementary diagrams and  $\hat{\mu}_\sigma$  is obtained by imposing the normalization property  $\sum_{\mathbf{k}} n_\sigma(\mathbf{k}) = \rho_\sigma$ .

In infinite dimensions  $\hat{\Sigma}_\sigma^*$  is different from zero only for  $\mathbf{r} = 0$ ,<sup>4</sup> so that the above procedure leads to an exact result for the double occupancy and the momentum distribution. In fact, in the limit  $D \rightarrow \infty$ , the behavior of the exchange operator is  $\hat{\rho}_\sigma(i,j) \sim \delta(\mathbf{r}_{ij}) + \frac{\text{const}}{\sqrt{2D}} \delta(\mathbf{r}_{ij} - \mathbf{a}) + \mathcal{O}(\frac{1}{D})$ , which trivially follows from the sequential relation, satisfied by the exchange operator. Because the exchange correlations form closed loops, the contributions to GHNC diagrams coming from  $\hat{\rho}_\sigma(\mathbf{r}_{ij} \neq 0)$  vanish as  $1/D$ . In the infinite-dimensional Hubbard model the nearest-neighbor hopping integral must be properly scaled,<sup>4</sup> since the kinetic energy  $T/N = -2Dt\hat{\rho}_\sigma(\mathbf{a}) \sim \sqrt{D}t$ . It follows that the GHNC diagrams shrink in their irreducible points and then  $\hat{\Sigma}_\sigma^*(i,j)$  is different from zero only for  $i = j$ , as seen from Eq. (5). In the

$D = \infty$  PM case,  $\hat{\Sigma}_\sigma^*(i)$  is independent of  $\mathbf{r}_i$  due to the translational invariance,  $\hat{\Sigma}_\sigma^*(\mathbf{k})$  becomes a constant and can be easily calculated. For instance, at  $\rho_\sigma = \rho/2$ ,  $\hat{\Sigma}_\sigma^* = [-1 + \sqrt{1 + (g^2 - 1)(2 - \rho)\rho}]/(2 - \rho)$ .

In any finite dimension,  $\hat{\Sigma}_\sigma^*(\mathbf{k})$  is not a constant. Neglecting  $\hat{\Sigma}_\sigma^{\text{GHNC}}$  in Eq. (9) is equivalent to the well-known Gutzwiller approximation (GA). The inclusion of  $\hat{\Sigma}_\sigma^{\text{GHNC}}$  obviously improves the GA and moreover goes beyond other recently proposed approximation schemes, like that of Refs. 13 and 14, based on an expansion of  $\hat{\Sigma}_\sigma^*$  around its  $D = \infty$  value, and that of Ref. 15 practically limited for the low-dimensional case.

Figures 2–4 report the results obtained for the Hubbard model in the 2D PM case at half- and quarter-filling, by including elementary diagrams, along the GHNC-n scheme up to the fourth order, in the calculation of  $\hat{\Sigma}_\sigma^*(k,j)$ , appearing in Eq. (9). The GA and variational Monte Carlo (VMC) (Ref. 10) results are also reported for comparison. Figure 2 shows the double occupancy  $d$ , the kinetic energy  $T/Nt$ , and the total energy for  $U/t = 6$ , at half-filling, as a function of the Gutzwiller parameter  $g$ . The energies at half- and quarter-filling are displayed versus the coupling constant  $U/t$  in Fig. 3. In addition, Fig. 4 displays the  $k$ -dependent momentum distribution at  $\rho = 1, 0.5$  for  $U/t = 8$ . Other  $k$ -dependent quantities are in principle calculable and will be presented elsewhere.<sup>12</sup> At  $D = \infty, \rho = 1$  the present scheme coincides with the GA and has therefore the same spurious metal-insulator transition at a finite  $U_c$ .<sup>13,14</sup> For  $D = 2$ , however, it is apparent from Figs. 2 and 3, that this transition has disappeared. A more detailed discus-

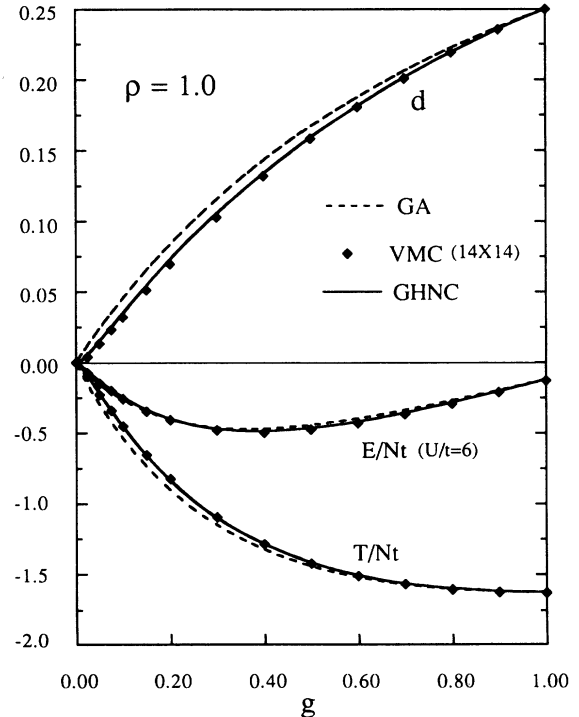


FIG. 2. Double occupancy and kinetic energy at half-filling, as a function of  $g$  for the 2D PM case. The total energy is given for  $U/t = 6$ , and is variationally minimized for  $g_0 = 0.42$ .

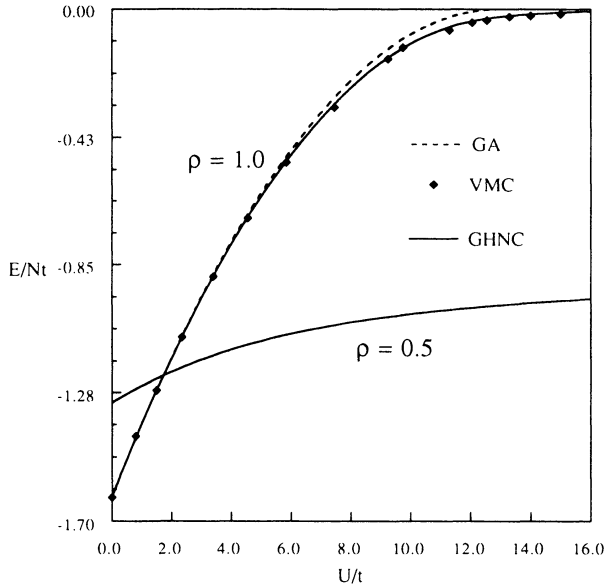


FIG. 3. Total energy at half- and quarter-filling, as a function of the coupling constant.

sion of the double occupancy as a function of  $U$  for higher  $D$  will be given elsewhere.<sup>12</sup> The GHNC results are very close to the VMC results in the whole range of the coupling constant. Such a GHNC approximation works extremely well for the 1D PM case also, where it provides energy estimates,<sup>12</sup> in very good agreement with the exact solution.<sup>5</sup> Results of similar quality are expected for other Gutzwiller correlated trial functions as well.

In conclusion, we have presented a FHNC scheme, called GHNC, specialized for Gutzwiller correlated wave functions, where the Pauli principle violations of the standard FHNC theory are completely removed at any level of approximation. For the one- and infinite-dimensional PM cases, the exact analytical results by Metzner and Vollhardt<sup>3,4</sup> are recovered. More generally, the GHNC equations can be solved by approximating the elementary diagrams. A suitable approximation scheme for the elementary diagrams has been found, which provides very good results for the 1D (Ref. 12) and 2D Hubbard model. The method may be applied for different

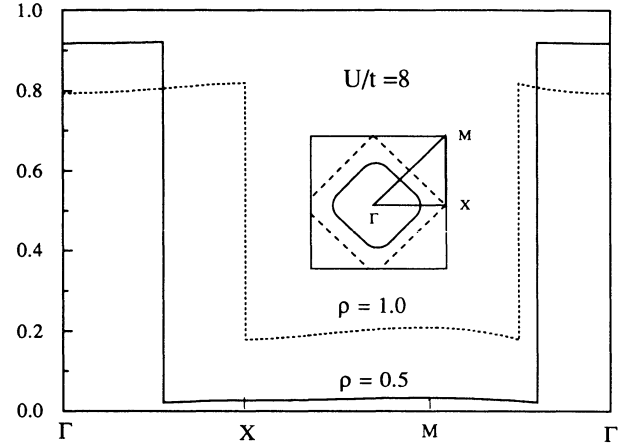


FIG. 4. Momentum distribution for the 2D PM case. The optimal values  $g = 0.25$  and  $0.40$  have been used for  $\rho = 1$  and  $0.5$ , respectively.

model functions  $|\Phi_0\rangle$ , such as SDW, BCS, etc., irrespective of dimensionality. The present GHNC scheme can also be used to evaluate nondiagonal matrix elements of the Hamiltonian and the identity operator and, should be particularly useful for CBF-type calculations. Such matrix elements can be calculated exactly at  $D = \infty$ , which may be useful to go beyond the variational theory for the infinite-dimensional Hubbard model. Work in this direction is in progress. Finally, we believe that the GHNC scheme can also be extended to more structured correlation operators. For instance, in the case of Jastrow correlated wave functions, the correlation operator  $\hat{f}(\mathbf{r}_{ij})$  can be considered as a product of a Gutzwiller operator  $\hat{f}_G$  and a smooth long-range correlation  $\hat{f}_L(\mathbf{r}_{ij}) \cdot \hat{f}_L(\mathbf{r}_{ij})$  can be treated by ordinary FHNC reasonably well, while GHNC can take care of the short-range part very accurately.

We are grateful to H. Shiba and H. Yokoyama for kindly providing us with their VMC data for comparison. Part of this work was sponsored through the Istituto Nazionale di Fisica della Materia (INFM) and the European Research Office of the U.S. Army.

<sup>1</sup> S. Fantoni, X.Q. Wang, E. Tosatti, and L. Yu, *Physica C* **153**, 1255 (1988); X.Q. Wang, S. Fantoni, E. Tosatti, L. Yu, and M. Viviani, *Phys. Rev. B* **41**, 11 479 (1990).

<sup>2</sup> X.Q.G. Wang, S. Fantoni, E. Tosatti, and L. Yu, *Phys. Rev. B* **46**, 8894 (1992).

<sup>3</sup> W. Metzner and D. Vollhardt, *Phys. Rev. Lett.* **59**, 121 (1987); F. Gebhard and D. Vollhardt, *ibid.* **59**, 1472 (1987).

<sup>4</sup> W. Metzner and D. Vollhardt, *Phys. Rev. Lett.* **62**, 324 (1989).

<sup>5</sup> S. Fantoni and S. Rosati, *Nuovo Cimento* **20A**, 179 (1974); **25A**, 593 (1975); S. Fantoni, *ibid.* **44A**, 191 (1978).

<sup>6</sup> A. Fabrocini and S. Fantoni, *First International Course on Condensed Matter*, ACIF series Vol. 8, edited by D. Prospero, S. Rosati, and G. Violini (World Scientific, Singapore, 1986), and references therein.

<sup>7</sup> J.E. Hirsch, *Phys. Rev. B* **31**, 4403 (1985); S. Sorella, S. Baroni, R. Car, and M. Parrinello, *Europhys. Lett.* **8**, 663 (1989).

<sup>8</sup> N. Trivedi and D.M. Ceperley, *Phys. Rev. B* **41**, 4552 (1990); K.J. Runge, *ibid.* **45**, 7229 (1992).

<sup>9</sup> E. Dagotto and A. Moreo, *Phys. Rev. Lett.* **63**, 2148 (1989); A. Parola, S. Sorella, M. Parrinello, and E. Tosatti, *Phys. Rev. B* **43**, 6190 (1991).

<sup>10</sup> H. Yokoyama and H. Shiba, *J. Phys. Soc. Jpn.* **56**, 1490 (1987); **56**, 3570 (1987); **56**, 3582 (1987); **59**, 3669 (1990); C. Gros, R. Joynt, and T.M. Rice, *Phys. Rev. B* **36**, 381 (1987).

<sup>11</sup>  $\tilde{g}(\mathbf{r})$  is defined here with a factor  $\rho^2/2$  as compared with Refs. 5 and 6. See Ref. 12 for more details.

<sup>12</sup> X.Q.G. Wang, Ph.D. thesis, SISSA, Trieste, 1992; X.Q.G. Wang and S. Fantoni (unpublished).

<sup>13</sup> W. Metzner, *Z. Phys. B* **77**, 253 (1989).

<sup>14</sup> F. Gebhard, *Phys. Rev. B* **41**, 9452 (1990).

<sup>15</sup> Y.M. Li and N. D'Ambrumenil, *Phys. Rev. B* **46**, 13928 (1992).